Proceedings Paper:
Criado, M, Mundra, S, Bernal, SA et al. (2018) Influence of sulfide on the onset of chloride-induced corrosion of steel reinforcement in alkali-activated slags. In: Basheer, PAM, (ed.) Durability of Concrete Structures. ICDCS2018: 6th International Conference on Durability of Concrete Structures, 18-20 Jul 2018, Leeds, UK. Whittles Publishing. Article no: 1241, pp. 149-153. ISBN: 978-184995-394-8.

Sixth International Conference on the Durability of Concrete Structures **Paper Number 1241**
18-20 July 2018
University of Leeds, Leeds, West Yorkshire, LS2 9JT, United Kingdom

Influence of Sulfide on the Onset of Chloride-Induced Corrosion of Steel Reinforcement in Alkali-Activated Slags

M. Criado, S. Mundra, S.A. Bernal, J.L. Provis
Department of Materials Science and Engineering, The University of Sheffield, Sir Robert Hadfield Building, Sheffield, S1 3JD, United Kingdom

ABSTRACT

In alkali-activated slags (AAS), where ground granulated blast furnace slag is used as the main precursor, the presence of reduced sulfur species yields a highly reducing pore solution environment. This study investigates the influence of sulfide on steel passivation in alkali-activated slag mortars immersed in alkaline (1 M NaOH) and alkaline chloride-rich (1 M NaOH with 5 M NaCl) solutions, and the dependency of chloride-induced pitting on the immersion time and the concentration of sulfide in simulated alkali-activated slag pore solutions (containing 0.80 M OH^- and 0 M, 0.01 M and 0.45 M HS^-) by means of electrochemical techniques. Surface-sensitive X-ray photoelectron spectroscopic (XPS) and Raman spectroscopic analysis of the corrosion products formed on the steel surfaces, both in alkali-activated slag mortars and in simulated pore solutions, shows that sulfide has a very important influence in altering – but not necessarily in a deleterious way – the characteristics of the steel surface under these conditions.

Keywords: alkali-activated slags; simulated pore solution; corrosion; chloride; sulfide; XPS

INTRODUCTION

The increasing demand for sustainable concretes, and for concretes with specialised performance characteristics, has promoted the development of a class of alternative binders called alkali-activated slags (AAS) (Provis et al., 2015). To form this type of binder, ground granulated blast furnace slag sourced from the ironmaking industry, is reacted with an alkaline solution to form a hardened product. Their manufacture can achieve significant reductions in greenhouse emissions, and also brings performance advantages in some applications, compared to Portland cement (PC) (Gartner and Macphee, 2011).

Corrosion of reinforcing steel is one of the main causes for the failure of reinforced concrete structures. Steel rebars embedded in PC-based concretes are protected from corrosion by a thin oxide film that is formed and maintained on rebar surfaces due to the high pH level of the surrounding concrete, unless the film is damaged by the presence of chloride ions (Angst et al., 2017). The reaction products, the pore network microstructure and the pore solution composition in AAS vary significantly from those encountered in PC-based cements (Lloyd et al., 2010). Therefore, differences in mechanisms of steel reinforcement corrosion could be expected for both systems.

Among the minor elements present in slags that have been used to produce alkali-activated cements, sulfur must be viewed carefully regarding electrochemical interactions, as it is a redox-sensitive element. The main oxidation state of sulfur in blast furnace slag is sulfide (-2 oxidation state), which is released into the alkaline aqueous solution as the slag dissolves during alkali-activation (Gruskovnjak et al., 2006). The presence of sulfide in an electrolyte solution alters the nature of the passive film formed on a carbon steel surface in contact with the solution, which is expected to directly impact the mechanism of chloride-induced corrosion.

The aim of this study is to investigate the influence of sulfide on steel passivation in alkali-activated slag mortars immersed in alkaline and alkaline chloride-rich solutions, and the dependency of chloride-induced pitting on the immersion time and the concentration of sulfide in simulated alkali-activated slag pore solutions. This is investigated by electrochemical techniques, and X-ray photoelectron spectroscopy (XPS) and Raman spectroscopy are used to characterise the corrosion products formed on the steel surfaces, both in slag mortars and in simulated pore solutions.

EXPERIMENTAL METHODOLOGY

Materials and Environments

Mild steel flat bars (95 mm x 15 mm) were obtained from a local supplier in Sheffield, UK, and small pellets (diameter 12 mm and thickness 5.5-6.5 mm) were also cut from these rebars for some tests. The chemical composition of the steel (% by weight) is 0.21 C, 0.23 Si, 0.76 Mn, 0.04 P, 0.03 S, 0.13 Cr, 0.20 Ni, 0.47 Cu, 0.02 Mo, and balance Fe. In some tests, flat coupons of mild steel were used instead of the bars. Prior to electrochemical testing, the as-received steel was embedded in mortars, with ends masked with an epoxy resin to leave an exposed surface area of 6 cm^2, while the pellet surfaces were polished using SiC abrasive paper with 240 to 600 grit sizes and degreased using acetone, leaving an exposed surface area of 0.287 cm^2 for the simulated pore solution tests.

A commercial powdered blast furnace slag supplied by ECOCEM® France was used to produce the mortar blocks, with chemical composition (% by weight) 41.8 CaO, 36.0 SiO_2, 11.3 Al_2O_3, 6.5 MgO, 0.7 SO_3, 0.3 Fe_2O_3, 0.5 TiO_2, 0.3 MnO, 0.4 K_2O and 1.95 loss on ignition at 1000°C. The activator used for preparation of alkali-activated slag mortar specimens was prepared by mixing commercial sodium metasilicate powder (Sigma-Aldrich, Na_2SiO_3) into distilled water until complete dissolution was reached. Blast furnace slag was activated with 7 wt.% sodium metasilicate, at an activator to total binder (anhydrous slag + anhydrous sodium metasilicate) ratio of 0.40.

Prismatic mortar specimens were prepared with dimensions of 80x50x50 mm, each containing two flat mild steel bars. After 24 h the mortars were demoulded, sealed with cling film and stored at 20±2°C for 6 days, and then immersed totally in 1 M NaOH solution or in 1 M NaOH + 5 M NaCl solution for 180 days. Duplicate mortar specimens were made for each mortar/steel system, giving four test bars for each condition.

The simulated pore solutions contain 0.80 M NaOH and 0 M, 0.01 M and 0.45 M HS^- ($Na_2S{\cdot}9H_2O$, Sigma Aldrich). The steel specimens were exposed to the simulated pore solutions for a maximum duration of 28 days.

Electrochemical Testing

For mortars, corrosion potential (E_{corr}) measurements were recorded periodically up to 180 days and polarization curves were measured after 180 days of immersion in each environment. During the measurements, an external stainless steel cylinder of 5 cm diameter carrying a centrally drilled hole and an Ag/AgCl (filled with 3 M KCl) positioned in the hole were used as counter and reference electrodes, respectively. A wet pad was interposed between these electrodes and the mortar surface to make the electrochemical measurements possible. A Princeton Applied Research VersaSTAT 3F was utilised for the electrochemical measurements. Ohmic drop-compensated anodic polarisation curves were recorded at a scan rate of 0.1667 mV s^{-1}.

In simulated pore solutions, the measurements were conducted using a conventional three electrode setup: a stainless steel counter electrode, an Ag/AgCl (filled with 3 M KCl) reference electrode, and the steel surface acting as the working electrode. The reference electrode was positioned near the surface of the working electrode using a Luggin capillary. All measurements were conducted at room temperature (22 ± 2 °C) on at least two replicate samples, in a 400 mL corrosion cell, using a PGSTAT 204 potentiostat/galvanostat (Metrohm Autolab B.V.). E_{corr} was recorded for 30 mins at the beginning of the experiment, unless the change in potential with time (dV/dt) reached ≤ 1 µV/s before 30 mins.

The chloride threshold was determined using anodic polarisation conducted with scan rate of 0.167 mV s^{-1} and step potential 0.244 mV. Abrupt spikes in the current density during the anodic sweep were considered to be representative of pitting.

Corrosion Product Analysis

Surface-sensitive X-ray Photoelectron Spectroscopy (XPS)

The analyses were carried out using a Kratos Ultra instrument with a monochromated aluminium source, and three analysis points per sample. The survey scans were collected between 1200 to 0 eV binding energy, at 160 eV pass energy, 1 eV intervals, and 300 s/sweep with two sweeps being collected. The data can then be quantified using theoretical Schofield relative sensitivity factors.

Raman Spectroscopy

Raman measurements were taken using a Renishaw InVia Raman Microscope equipped with a 514.5 nm laser, a Leica microscope, and 50x magnification objective lenses. The laser power was 1 mW, the integration time was 15 s, and 3 accumulations were used. The Raman shift was calibrated to the silicon peak at 520 cm^{-1}.

RESULTS AND DISCUSSION

Influence of Sulfide on Steel Passivation in Alkali-Activated Slag Mortars

Figure 1 shows E_{corr} values for the steels embedded in alkali-activated slag mortars immersed in alkaline and alkaline rich-chloride solutions. Initially in both solutions, E_{corr} was -0.285 V vs. Ag/AgCl, this potential value decreased drastically by increasing the immersion time. After 5 days, E_{corr} was more

negative than -0.550 V vs. Ag/AgCl and these values became more negative with time, reaching values of -0.633 and -0.636 V vs. Ag/AgCl when immersed in NaOH and NaOH-NaCl solutions respectively, at the end of the test.

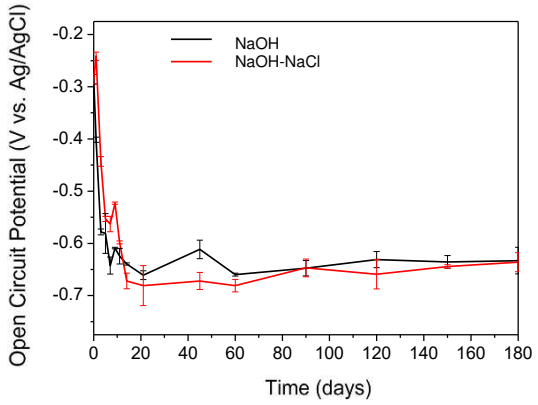

Fig. 1. Corrosion potential as a function of time for steel embedded in AAS mortars immersed in NaOH and NaOH-NaCl solutions.

The slag contains sulfide, which is released during its dissolution when contacting the alkaline activator. The dissolved sulfide induces a reducing internal environment in the AAS mortars and a decrease in the amount of dissolved oxygen within the pore solution, driving the redox potential of the embedded steel reinforcement towards more negative values (Criado et al., 2018; Glasser, 2001), Fig. 1. In the case of steel embedded in slag mortars immersed in the NaOH-NaCl solution, the decrease of the potential would classically be interpreted as being due to the breakdown of the passive film induced by the chloride ions. However, the fact that this is so similar to the results obtained in the absence of chloride indicates that it is more likely to be due to the highly reducing conditions at the steel-concrete interface imposed by the presence of sulfide ions.

Figure 2 shows anodic polarisation curves recorded on the flat steel bars embedded in slag mortars exposed to these same two immersion environments for 180 days.

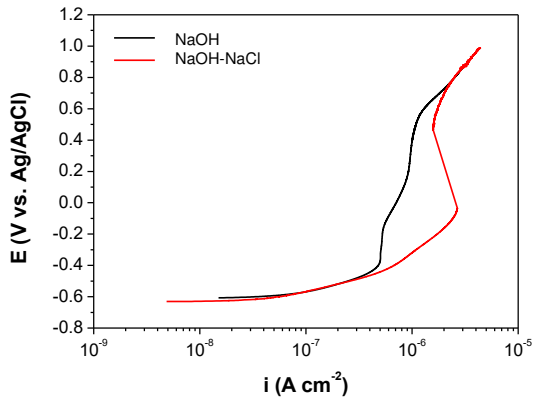

Fig. 2. Anodic polarisation curves recorded for steel embedded in AAS mortars immersed in NaOH and NaOH-NaCl solutions.

The anodic polarisation curves showed E_{corr} values around -0.607 and -0.630 V vs. Ag/AgCl and corrosion current density (i_{corr}) values of 0.2 and 0.3 μA cm^{-2} for the steel immersed in NaOH and NaOH-NaCl solutions respectively. The very negative values of potential indicated that the sulfide from the slag reduced the redox potential around the steel bars, while the i_{corr} values indicated a low corrosion level (Andrade et al., 1986). In NaOH-NaCl solution, the polarisation curve showed an active/passive transition potentials in the range -0.350 to -0.150 V vs. Ag/AgCl, probably ascribed the transformation of S^{2-} .

Time- and Concentration-Dependent Chloride-Induced Pitting in Simulated AAS Pore Solutions

In the case of simulated pore solutions representative of AAS (0.80 M OH^- + 0.45 M HS^-), the E_{corr} was found to be influenced by time and varied between -0.550 V and -0.705 V (as seen in Figure 3). Figure 3 shows the influence of the dissolved sulfide on the E_{corr}. An increase in the sulfide content in the aqueous electrolyte resulted in an increase in the reducing nature of the metal/electrolyte interface. The E_{corr} values observed in simulated pore solutions are in good agreement with those determined for AAS mortars (Figure 1).

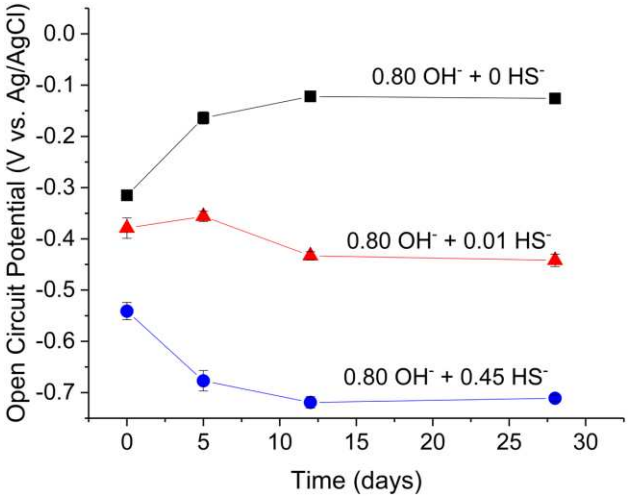

Fig. 3. E_{corr} values recorded for steel immersed in alkaline solutions (0.80 M OH^-) with varying concentrations of HS^- (0, 0.01 and 0.45 M).

The highly negative E_{corr} values observed for steel exposed to solutions containing 0.01 M and 0.45 M HS^- are once again attributed to the reducing nature of the sulfide and the depletion of oxygen (Mundra et al., 2017). Consequentially, passivation of the steel reinforcement by an iron oxide film is hindered, and instead a surface layer composed of $Fe(OH)_2$ and Fe sulfide compounds is formed (Mundra et al., 2017).

Table 1 shows the variation in chloride content (represented as threshold Cl/OH molar ratio) required to induce steel corrosion in different simulated pore solutions, as a function of the length of time for which

the steel was exposed to the aqueous environment before addition of the chloride. It can be clearly seen that the concentration of sulfide in the pore solution and the time of exposure play a critical role in the initiation of chloride induced pitting on the surface of steel rebar. In the case of simulated pore solution of AAS (0.80 M OH^- + 0.45 M HS^-), localised corrosion due to chloride was not observed at all under these conditions.

Table 1. Chloride threshold values as a function of the concentration of HS^- in the simulated pore solution, and the duration of exposure of the steel to the solution prior to chloride addition. P and NP stand for pitting and no pitting respectively, and the numbers in the parentheses depict the chloride threshold value in the form of $[Cl^-]/[OH^-]$. The solution containing 0.45 M HS^- is designated as representing AAS pore solution.

Test solution	0 d	5 d	12 d	28 d
0.80 M OH^- + 0.01 M HS^-	P (2.5)	P (3)	P (2.8)	P (2)
0.80 M OH^- + 0.09 M HS^-	P (3.1)	P (3)	NP	NP
0.80 M OH^- + 0.45 M HS^-	NP	NP	NP	NP

Corrosion Product Analysis

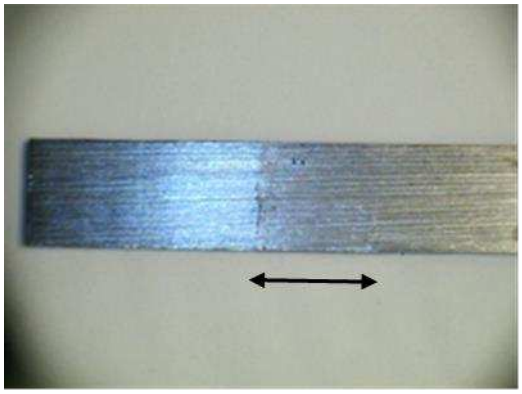

Fig. 4. Image of steel bar extracted from AAS mortar after 180 days of immersion in NaOH-NaCl solution.

Fig. 4 shows a photograph of the surface aspect of a flat steel bar extracted from a slag mortar that had been immersed in NaOH-NaCl solution for 180 days. The steel showed a thin mortar layer adhering tightly to its surface (which prevented effective analysis of the underlying steel by XPS, and could not be removed by ion sputtering), but no evidence of pits or a corrosion products layer. A similar appearance was observed for the steel extracted from the mortar that had been immersed in NaOH solution without chloride (not shown).

However, a Raman spectrum of the film was able to be collected, Figure 5. The Raman results for the rebars extracted from mortars that had been exposed to the NaOH and NaOH-NaCl solutions were similar and the only ordered compound identified by sharp Raman peaks was calcite ($CaCO_3$); all of the observable peaks could be aligned with the results for this phase in the literature (Wehrmeister et al., 2010). Corrosion products were not found on the steel surfaces.

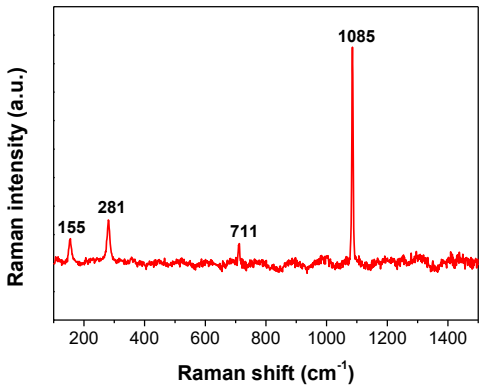

Fig. 5. Raman spectrum of the film detected on the steel surface shown in Figure 4.

However, the composition of the passive film on steel immersed in simulated alkali-activated slag pore solutions was able to be determined using XPS, as there was no adhering mortar layer. Figure 6 shows that the existence of Fe^{2+} species was more prominent than the more usual Fe^{3+} in passivating oxide film. The steel surface was rich in various Fe-S species, which (according to the results in Table 1) had evidently altered the critical chloride level.

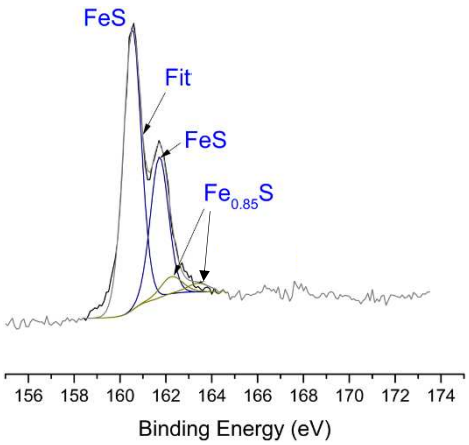

Fig. 6. Fe_{2p} XPS results for the passive film formed on steel after immersion in simulated alkali-activated slag pore solution (0.80 M NaOH + 0.45 M Na_2S).

CONCLUSIONS

The presence of sulfide ions in alkali-activated slag mortars produced a reducing environment, leading a decrease of corrosion potential values of steel reinforcement. However, the corrosion current density values indicated a low corrosion level and high resistance to corrosion processes in the presence of chloride ions. Studies conducted in simulated pore solutions complemented the argument that a highly reducing environment is

prevalent in AAS due to the high concentration of dissolved sulfur species in the reduced state. Localised corrosion due to chloride was not evident in simulated pore solutions representative of AAS. The chloride threshold values required to induce steel corrosion were dependent on the concentration of sulfide and the duration of exposure to sulfide-rich solution prior to addition of chloride.

The steel reinforcements exposed to simulated pore solutions were observed to possess a layer of Fe(II)-S complex. The steel bars extracted from slag mortars showed a strongly mortar, but no corrosion products were detected even in the presence of chloride ions.

Acknowledgements

The research leading to these results received funding from the European Research Council under the European Union's Seventh Framework Programme (FP/2007-2013) / ERC Grant Agreement #335928. The authors would like to acknowledge the input of Dr. Deborah B Hammond (Sheffield Surface Analysis Centre, The University of Sheffield) in the XPS work. This research was performed in part at the MIDAS Facility, at The University of Sheffield, which was established with support from the UK Department of Energy and Climate Change.

References

Andrade, C., Castelo, V., Alonso, C., Gonzalez, J.A., 1986. The determination of the corrosion rate of steel embedded in concrete by the polarization resistance and AC impedance methods, in: V. Chaker et al., ASTM STP906, Corrosion Effect of Stray Currents and the Techniques for Evaluating Corrosion of Rebars in Concrete. ASTM International, Philadelphia, pp. 43-63.

Angst, U.M. et al., 2017. The steel–concrete interface. Mater. Struct., 50(2): 143.

Criado, M., Bernal, S.A., Garcia-Triñanes, P., Provis, J.L., 2018. Influence of slag composition on the stability of steel in alkali-activated cementitious materials. J. Mater. Sci., 53: 5016-5035.

Gartner, E.M., Macphee, D.E., 2011. A physico-chemical basis for novel cementitious binders. Cem. Concr. Res., 41(7): 736-749.

Glasser, F., 2001. Mineralogical aspects of cement in radioactive waste disposal. Mineral. Mag., 65(5): 621-633.

Gruskovnjak, A., Lothenbach, B., Holzer, L., Figi, R., Winnefeld, F., 2006. Hydration of alkali-activated slag: comparison with ordinary Portland cement. Adv. Cem. Res., 18(3): 119-128.

Lloyd, R.R., Provis, J.L., van Deventer, J.S.J., 2010. Pore solution composition and alkali diffusion in inorganic polymer cement. Cem. Concr. Res., 40(9): 1386-1392.

Mundra, S. et al., 2017. Steel corrosion in reinforced alkali-activated materials. RILEM Techn. Lett., 2: 33-39.

Provis, J.L., Palomo, A., Shi, C., 2015. Advances in understanding alkali-activated materials. Cem. Concr. Res., 78A: 110-125.

Wehrmeister, U., Soldati, A., Jacob, D., Häger, T., Hofmeister, W., 2010. Raman spectroscopy of synthetic, geological and biological vaterite: a Raman spectroscopic study. J. Raman Spectrosc., 41(2): 193-201.